Journal of Alloys and Compounds 522 (2012) 19–24

Contents lists available at SciVerse ScienceDirect

Journal of Alloys and Compounds

journal homepage: www.elsevier.com/locate/jallcom

Photocatalytic water splitting by band-gap engineering of solid solution $Bi_{1-x}Dy_xVO_4$ and $Bi_{0.5}M_{0.5}VO_4$ (M = La, Sm, Nd, Gd, Eu, Y)

Qizhao Wang[a,b], Ning An[a], Ruijuan Mu[a], Hui Liu[c,*], Jian Yuan[b], Jianwei Shi[b], Wenfeng Shangguan[b,**]

[a] College of Chemistry and Chemical Engineering, Northwest Normal University, Key Laboratory of Eco-Environment-Related Polymer Materials, Ministry of Education, Lanzhou 730070, China
[b] Research Center for Combustion and Environment Technology, Shanghai Jiao Tong University, Shanghai 200240, China
[c] School of Metallurgical Science and Engineering, Central South University, Changsha 410083, China

ARTICLE INFO

Article history:
Received 29 August 2011
Received in revised form 3 January 2012
Accepted 3 January 2012
Available online 28 January 2012

Keywords:
$Bi_{1-x}Dy_xVO_4$
Water splitting
Hydrogen
Solid solution
Ultraviolet light

ABSTRACT

A series of metal oxide solid solutions $Bi_{1-x}Dy_xVO_4$ and $Bi_{0.5}M_{0.5}VO_4$ (M = La, Sm, Nd, Gd, Eu, Y) were synthesized by solid state reaction at high temperature and characterized by XRD, UV–vis DRS, BET, SEM. $Bi_{1-x}Dy_xVO_4$ showed two crystal structures with the component content. For $0.3 \le x \le 1.0$, the structure was tetragonal type, while that was monoclinic when $x = 0$. For $0.1 \le x < 0.3$, tetragonal and monoclinic structures had been observed. $Bi_{1-x}Dy_xVO_4$ solid solutions of tetragonal type could split water into H_2 and O_2 simultaneously when loaded with 0.3 wt% Pt and 1 wt% Pt-Cr_2O_3 respectively as cocatalyst. Among these catalysts, $Bi_{0.5}Dy_{0.5}VO_4$ showed the best photocatalytic activity for water splitting under UV light irradiation. Besides, $Bi_{0.5}M_{0.5}VO_4$ (M = La, Sm, Nd, Gd, Eu, Y) were also prepared and discovered to be of tetragonal type as same as $Bi_{0.5}Dy_{0.5}VO_4$. They performed high photocatalytic activities of splitting pure water into H_2 and O_2 under UV light irradiation when loaded with 1 wt% Pt-Cr_2O_3. The activities of $Bi_{0.5}M_{0.5}VO_4$ (M = Dy, La, Sm, Nd, Gd, Eu, Y) solid solutions indicated band-gap engineering of metal oxide solid solutions was the feasible method to obtain a photocatalyst for overall water splitting.

1. Introduction

Since the evolution of hydrogen and oxygen on an electrochemical cell under the irradiation of ultraviolet (UV) light was first reported by Fujishima et al. [1], photocatalytic water splitting into H_2 and O_2 by semiconducting catalysts has received much attention [2–5]. Recently, in order to take advantage of more sunlight belonging to visible light spectra, the hot topic of photocatalytic water splitting has changed from using UV light to visible light [6,7]. Some new photocatalysts were discovered to have the ability to absorb visible light. However, most of them could only produce H_2 or O_2 with the help of sacrificial reagents, such as $K_2La_2Ti_3O_{10}$, $BiVO_4$, ZrW_2O_8, $Sm_2Ti_2S_2O_5$ and $CuFe_2O_4$ [8–12]. For efficient water splitting into H_2 and O_2, the conduction band (CB) and valence band (VB) of the photocatalysts should meet the potential requirements of reduction and oxidation of H_2O simultaneously. Several strategies, such as metal-doping [13,14], nonmetal-doping [15,16], and solid solution [17,18] were proposed to control CB and VB of photocatalytic materials. Among them, band-gap engineering of solid solution had attracted much attention since its composition could be tuned in a wide range. Recently, $(Ga_{1-x}Zn_x)(N_{1-x}O_x)$ and $(Zn_{1+x}Ge)(N_2O_x)$ solid solutions had been found to split water completely under visible light [6,19,20], indicating that band-gap engineering of solid solution was a feasible and effective method to obtain suitable CB and VB for overall water splitting.

As we known, $BiVO_4$ was an excellent photocatalyst for producing O_2 from $AgNO_3$ aqueous solution [9,21], but it was unable to reduce H_2O to H_2 because of the redox potential of its CB lower than that of H_2O/H_2. So $BiVO_4$ could be selected as one candidate for solid solution preparation. Recently, we reported in communications that $BiYWO_6$, $Bi_{0.5}Dy_{0.5}VO_4$ and Bi–Y–V oxide solid solutions providing new stable valence band to make band gap narrow acted as the photocatalyst for overall water splitting into H_2 and O_2 [22–24]. In this paper, in order to adjust the band structure and photocatalytic property, a series of solid solution photocatalysts $Bi_{1-x}Dy_xVO_4$(BDV) were synthesized by partial substitution of Dy^{3+} for Bi^{3+} in $BiVO_4$ and discovered to have photocatalytic activities when BDV were loaded with cocatalyst. BDV ($x = 0.3, 0.5$) were discovered to split water into H_2 and O_2. Furthermore, $Bi_{0.5}M_{0.5}VO_4$ (M = La, Sm, Nd, Gd, Eu, Y) with tetragonal structure were synthesized and their photocatalytic activities were discussed and compared with the photocatalytic property of $Bi_{0.5}Dy_{0.5}VO_4$.

* Corresponding author.. Tel.: +86 731 8883 0875; fax: +86 731 8710 0171.
** Corresponding author. Tel: +86 21 34206020; fax: +86 21 34206372.
E-mail addresses: leolau1979@gmail.com (H. Liu), shangguan@sjtu.edu.cn, qzwang@nwnu.edu.cn (W. Shangguan).

0925-8388/$ – see front matter.
doi:10.1016/j.jallcom.2012.01.017

2. Experimental

2.1. Preparation and characterization

All the chemical reagents were of analytical-grade purity and were used without further purification. Samples of $Bi_{1-x}Dy_xVO_4$ with $x = 0$, 0.1, 0.2, 0.3, 0.5, 0.7, 0.9 and 1.0 were prepared by solid-state reaction. Bi_2O_3, Dy_2O_3 and NH_4VO_3 were used as raw materials and blended with stoichiometric proportions. BDV were prepared by calcining the mixture at 1073 K in air for 12 h and then at 1123 K for 12 h with an intermadiate regrinding process. The same method was applied to synthesize $Bi_{0.5}M_{0.5}VO_4$ (M = La, Sm, Nd, Gd, Eu, Y) with Bi_2O_3, La_2O_3, Sm_2O_3, Nd_2O_3, Gd_2O_3, Eu_2O_3, Y_2O_3 and NH_4VO_3 as raw materials. For loading cocatalyst Pt-Cr_2O_3, the samples were impregnated into the aqueous solution dissolving $H_2PtCl_6{\cdot}2H_2O$ and $Cr(NO_3)_3$, followed by evaporation-to-dryness at 353 K and then calcination at 623 K for 2 h to load 1.0 wt% Pt-Cr_2O_3. Other cocatalysts were loaded onto samples in the same method.

X-ray diffraction patterns (XRD) of the metal oxides prepared were recorded on a Rigaku X-ray diffractometer D/MAX-2200/PC equipped with Cu K_α radiation (40 kV, 20 mA). SEM image was obtained using JSM-6460. The BET surface areas of BDV powders were determined from N_2 adsorption–desorption isotherm on Quantachrome NOVA 1000-TS. UV–vis diffuse reflectance spectra were measured using Shimadzu UV-3100 spectrophotometer. The reflectance spectra were transformed to absorption intensity by using Kubelka–Munk method.

2.2. Measurement of photocatalytic activity

The photocatalytic reactions were carried out in a Pyrex photoreactor ($\lambda > 300$ nm) equipped with cooling water. About 0.2 g of photocatalyst powders were dispersed and suspended in an aqueous solution in the reactor under the vertical irradiation of a 300 W Xe lamp. The amounts of H_2 and O_2 evolution were measured by using a gas chromatography (QC-9101, 5 Å-coloum) with thermal conductivity detector (TCD) and Ar as carrier gas.

3. Results and discussion

3.1. Characterization of the BDV solid solutions

Fig. 1 showed the X-ray diffraction patterns of $Bi_{1-x}Dy_xVO_4$. Fig. 1A indicated the BDV solid solutions had two kinds of crystal structures with the different Dy^{3+} content: monoclinic structure and tetragonal structure. As $x = 0$ and $x = 1.0$, BDV were $BiVO_4$ and $DyVO_4$, which were well crystallized with the monoclinic and tetragonal, respectively. When $0 < x < 1.0$, BDV changed from monoclinic structure to tetragonal structure. As $0.3 \leq x < 1.0$, BDV were solid solutions and were the tetragonal type as $DyVO_4$, but BDV ($x = 0.1$, 0.2) were mixture of tetragonal and monoclinic structures. Furthermore, as shown in Fig. 1B from $x = 0.3$ to $x = 1.0$, each peak shifted to a higher angle nearly in proportion to x.

Fig. 2 showed the results of UV–vis diffuse reflectance spectrum (DRS) of BDV with different values for x. According to the absorption edges of BDV, the band gaps of BDV estimated from the onset were presented in Table 1. The band gap of $BiVO_4$ and $DyVO_4$ were estimated to be 2.31 and 3.44 eV, respectively. The steep absorption edge of the BDV ($x = 0.3$–0.9) were located in a position between those of $BiVO_4$ and $DyVO_4$, and the absorption spectra were blue-shifted gradually with the increasing of x. Furthermore, there were two kinds of absorption mechanism for light absorption in the BDV ($x = 0.3$–0.7). The strong and extensive absorption was the major transition and regarded as band gap. The right-side absorption in

Table 1
Band gaps, energy gaps and BET surface area of BDV ($0 \leq x \leq 1$).

Samples	Band gap (eV)	Energy gap (eV)	BET (m^2/g)
$BiVO_4$	2.31	–	0.60
$Bi_{0.9}Dy_{0.1}VO_4$	2.31	–	0.32
$Bi_{0.8}Dy_{0.2}VO_4$	2.34	–	0.25
$Bi_{0.7}Dy_{0.3}VO_4$	2.95	2.53	0.31
$Bi_{0.5}Dy_{0.5}VO_4$	3.01	2.61	0.26
$Bi_{0.3}Dy_{0.7}VO_4$	3.06	2.69	0.18
$Bi_{0.1}Dy_{0.9}VO_4$	3.26	–	0.20
$DyVO_4$	3.44	–	0.17

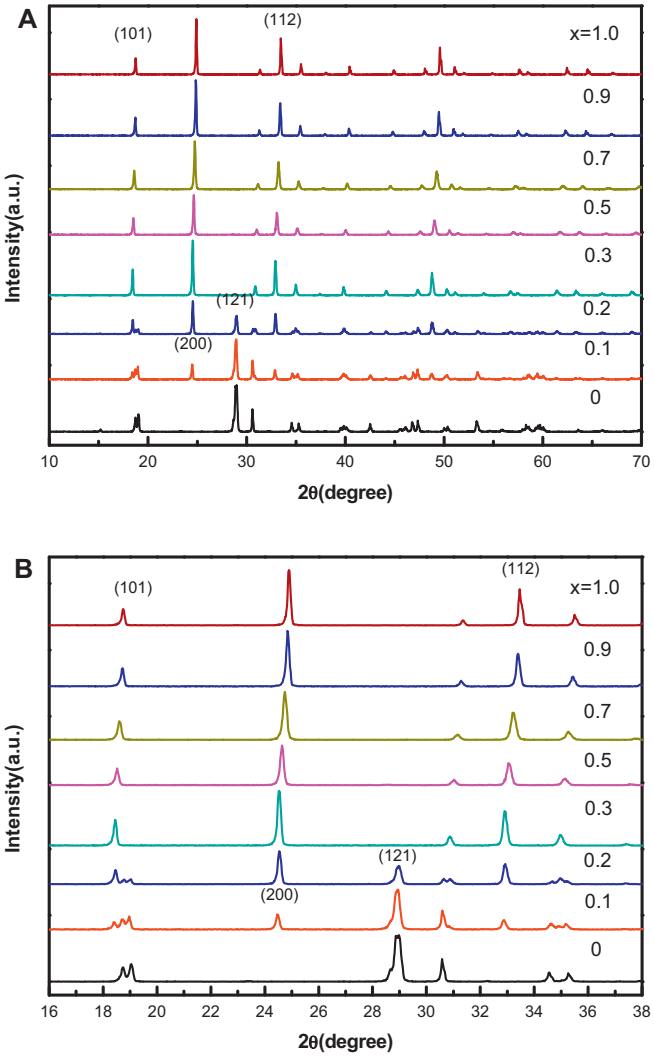

Fig. 1. X-ray diffraction (XRD) pattern for $Bi_{1-x}Dy_xVO_4$ ($x = 0$–1.0) measured over (A) a wide range and (B) a narrow range.

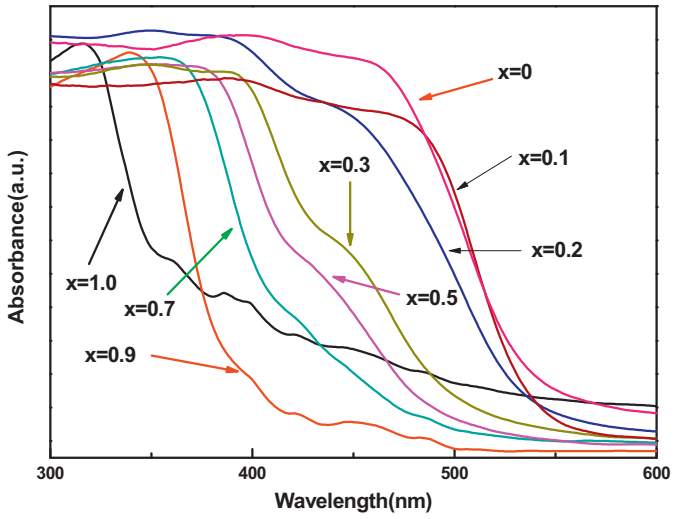

Fig. 2. UV–vis diffuse reflectance spectra of BDV.

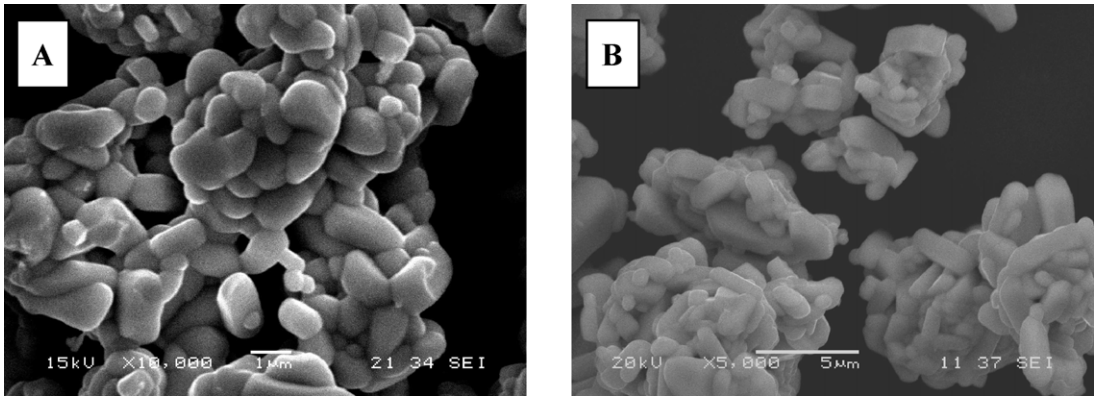

Fig. 3. SEM images of $Bi_{0.7}Dy_{0.3}VO_4$ (A) and $Bi_{0.5}Dy_{0.5}VO_4$ (B).

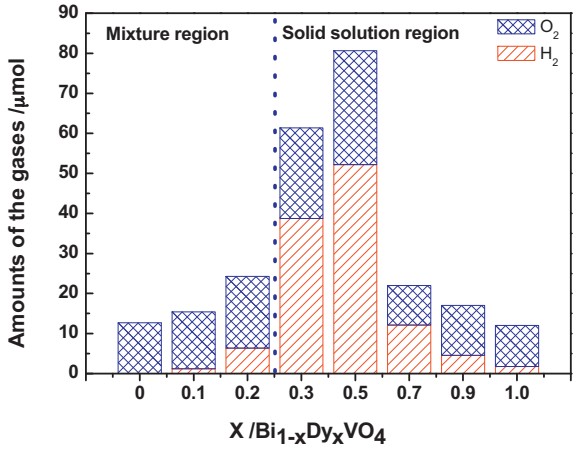

Fig. 4. Photocatalytic activity of BDV ($0 \le x \le 1$) for water splitting under UV ($\lambda > 300$ nm) light irradiation. Catalyst 0.2 g; 300 W Xe lamp as light source; determining and vacuumizing at the interval of 2 h.

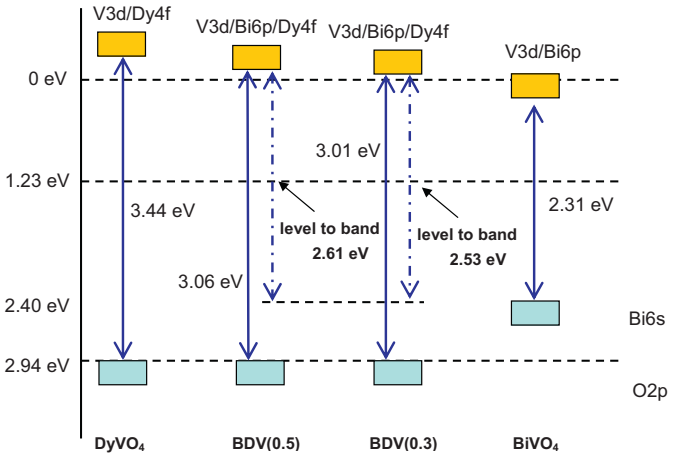

Fig. 6. Position of valence and conduction bands of BDV.

the low energy area should originate from the transition of energy level of Bi6s because Bi6s orbital cannot form band in tetragonal type structure. As shown in Figs. 1 and 2, BDV ($x = 0.3, 0.5$) solid solutions were single-crystal structures with tetragonal and capable of responding to visible light.

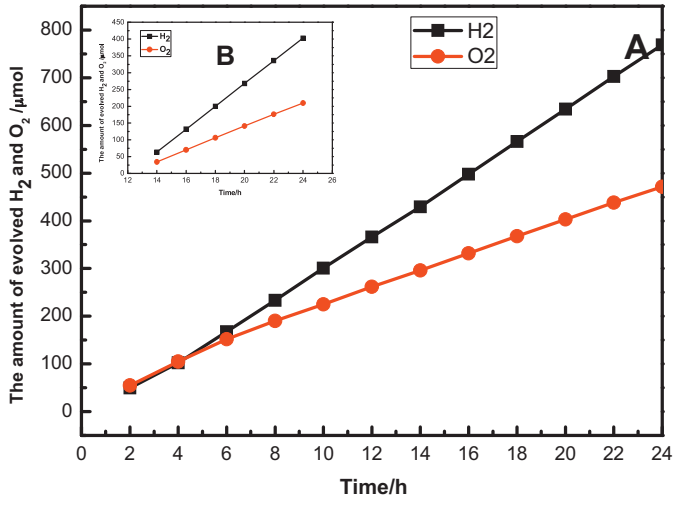

Fig. 5. H_2 and O_2 evolution by 1 wt% Pt-Cr_2O_3/BDV (0.5) under UV ($\lambda > 300$ nm) light irradiation. (A): H_2 and O_2 production from pure water on 1 wt% Pt-Cr_2O_3/BDV (0.5) in the period of 28 h; (B) after the reaction of 10 h under UV light irradiation. Catalyst 0.2 g; H_2O: 80 ml; 300 W Xe lamp as light source.

Table 1 showed the specific surface areas (SSA) of BDV ranged from 0.17 to 0.60 m^2/g, which were small because all the BDV were prepared by solid state reaction at high temperature, it was suggested that SSA should make no different effect on the activities of BDV. Fig. 3 showed the SEM photographs of BDV ($x = 0.3, 0.5$) solid solutions. Irregular-shaped particles with smooth surfaces were

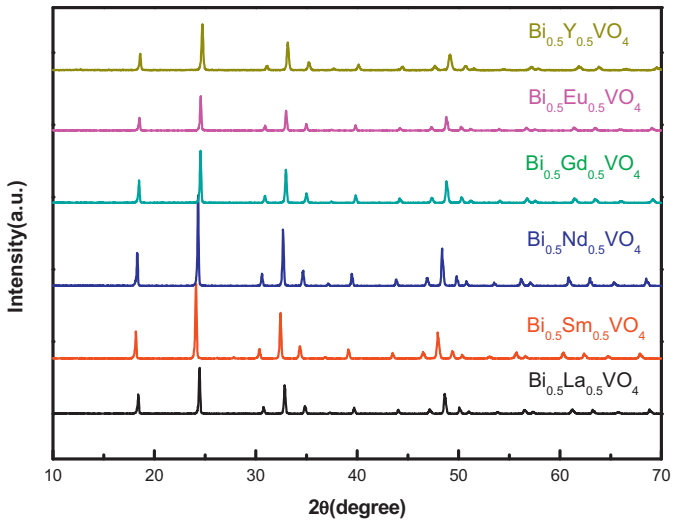

Fig. 7. X-ray diffraction (XRD) pattern for $Bi_{0.5}M_{0.5}VO_4$ (M = La, Sm, Nd, Gd, Eu, Y).

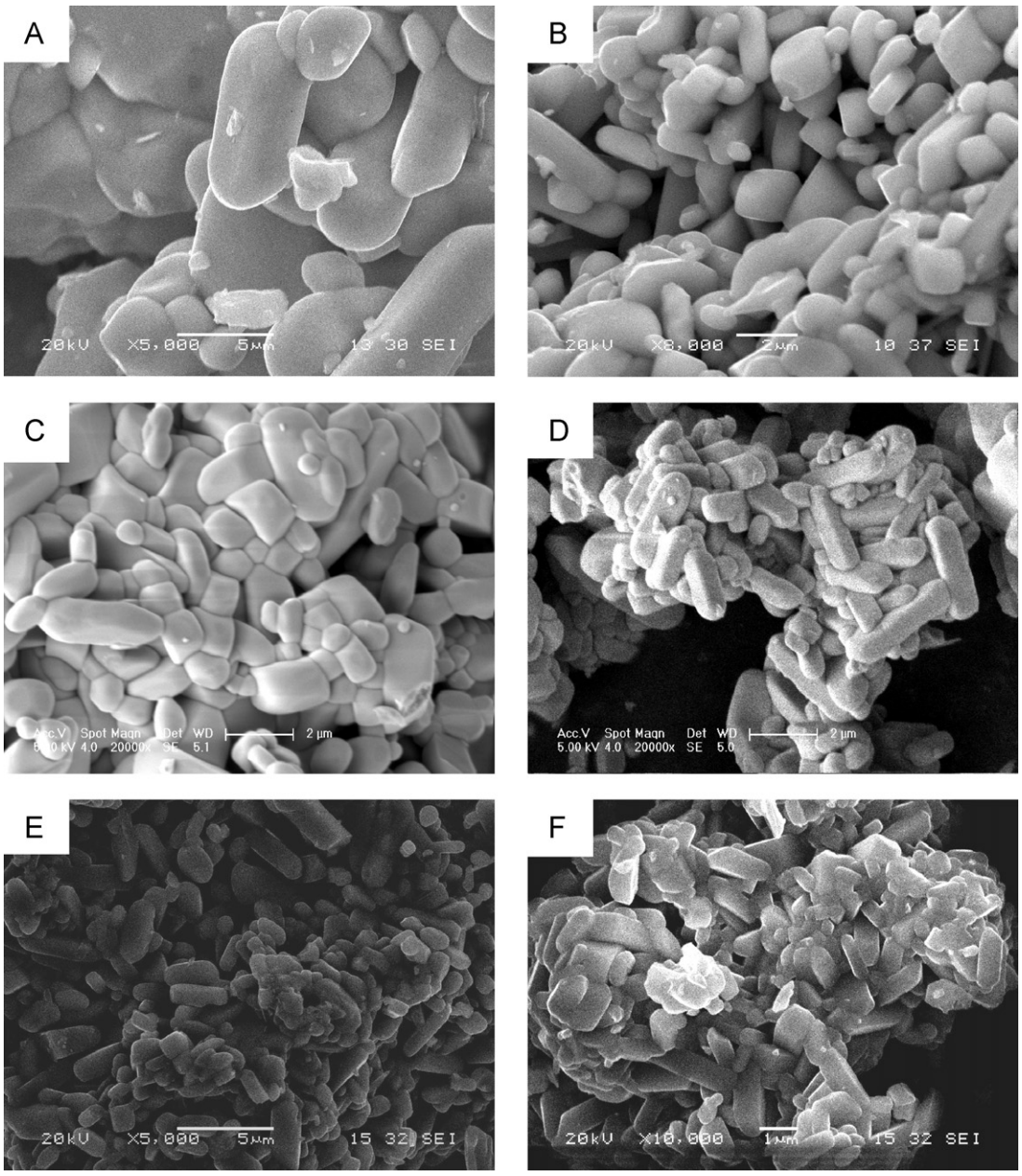

Fig. 8. SEM images of $Bi_{0.5}M_{0.5}VO_4$ (M = La, Sm, Nd, Gd, Eu, Y).

observed for BDV ($x = 0.3$, 0.5) and the average particle size was estimated as 1–3 μm in diameter.

3.2. Photocatalytic activity of the BDV solid solutions

Photocatalytic reactions indicated that the BDV without cocatalyst were unable to split pure water into H_2 and O_2. When cocatalyst such as Pt was loaded onto BDV, the samples worked as photocatalysts for hydrogen evolution from water under UV light irradiation. Fig. 4 showed H_2 and O_2 production from water on 0.3 wt% Pt/BDV as a function of x under Xe lamp irradiation. For $x = 0$, O_2 was only produced, and for $0 < x \leq 1.0$, the amounts of H_2 and O_2 produced by BDV firstly increased and then decreased. Among them, $Bi_{0.5}Dy_{0.5}VO_4$ showed the best photocatalytic activity for water splitting under UV light irradiation.

As we known from above research, we can conclude that $Bi_{0.5}Dy_{0.5}VO_4$ solid solutions were single phase with tetragonal structure. Furthermore, $Bi_{0.5}Dy_{0.5}VO_4$ was found to act as a photocatalyst for overall water splitting under UV light irradiation when loaded with 1 wt% Pt-Cr_2O_3. Fig. 5A showed the time course of H_2 and O_2 evolution from pure water on 1 wt% Pt-Cr_2O_3-coloaded BDV (0.5) (Pt-Cr_2O_3/BDV (0.5)) under UV light irradiation. As shown in Fig. 5A, the evolution of O_2 and H_2 was observed after the beginning of the reaction, but the rate of H_2 evolution increased gradually. The reason was that part of Cr (III) was oxidized into Cr (VI) when Cr_2O_3 was loaded on BDV (0.5). Therefore in the beginning of the reaction electrons were used to reduce Cr (VI) to Cr (III) and leaded to nonstoichiometrical H_2 and O_2. After 10 h reaction, the ratio of the mount of evolved H_2 to O_2 was about 2: 1, which meant BDV (0.5) can act as a photocatalyst for overall water splitting. Fig. 5B showed H_2 and O_2 production from pure water on 1 wt% Pt-Cr_2O_3/BDV (0.5) in the period after the reaction of 10 h under UV light irradiation [23]. As shown in Fig. 5B, 1 wt% Pt-Cr_2O_3/BDV (0.5) gave off stoichiometrical H_2 and O_2 from water under UV light irradiation. For

Table 2
Photocatalytic activity of BDV (0.5) loaded with 1 wt% Pt-Cr_2O_3 in the sacrificial reagent solutions. Catalyst 0.2 g; 300 W Xe lamp as light source; determining and vacuumizing at the interval of 2 h.

Catalyst	Wavelength (nm)	Sacrificial reagent[a]	H_2[b]	O_2[b]
$Bi_{0.5}Dy_{0.5}VO_4$	>300	Na_2SO_3	197.37	0
		$AgNO_3$	0	147.48

[a] Concentration of sacrificial reagent = 0.1 mol/L.
[b] Unit was μmol.

1 wt% Pt-Cr_2O_3/BDV (0.5), the amounts of the produced hydrogen and oxygen from water were about 67.46 μmol and 35.29 μmol for 2 h, respectively.

Sacrificial reagent solutions were often used to improve the photocatalytic ability of material. In order to avoid the effect of photolysis of sacrificial reagents in this study, sacrificial reagents of Na_2SO_3 solution and $AgNO_3$ solution were used to improve the H_2-producing and O_2-producing abilities of 1 wt% Pt-Cr_2O_3/BDV (0.5), respectively. Table 2 showed the amounts of H_2 and O_2 from sacrificial reagent Na_2SO_3 solution and $AgNO_3$ solution. The evolution rate of H_2 and O_2 on 1 wt% Pt-Cr_2O_3/BDV (0.5) was more higher than that for overall water splitting from water under UV light, respectively.

We know that the band structure of a photocatalyst, which can efficiently split water into H_2 and O_2 under UV light, should meet the potential requirements of reduction and oxidation of H_2O. As shown in Fig. 4, $BiVO_4$ loaded with 0.3 wt% Pt produced only O_2 under UV irradiation, but BDV (0.3, 0.5, 0.7, 0.9, 1.0) loaded 0.3 wt% Pt could split water into H_2 and O_2. Based on observed results of H_2 and O_2 evolution from pure water shown in Fig. 4, it can be concluded that the CB bottom level of $BiVO_4$ is more positive than that of H_2 evolution while the VB top level is more positive than that of O_2 evolution. But according to the BDV (0.3, 0.5, 0.7, 0.9, 1.0), the CB bottom level is more negative than that of H_2 evolution while the VB top level is more positive than that of O_2 evolution.

On the other hand, we think the band structure of BDV is similar to $InMO_4$ (M = V, Nb and Ta) [25] and $BiVO_4$. The CB of BDV should be composed of hybrid orbital of V 3d and Dy 4f, and the contribution of Dy 4f orbital to the conduction band might increase with the increasing content of Dy ions in the solid solutions. As reported by Scaife [26], the top of the valence band should be at 2.94 V versus NHE in the case of oxides without partly filled electrons. Therefore, the conduction band minimum of BDV (0.5) with 3.01 eV band gap should be around 0.08 V. This position is higher than H_2/H_2O potential and suggests that BDV (0.5) has the potential to reduce H_2O toH_2. Other BDV (x = 0.1, 0.2, 0.3, 0.7, 0.9) solid solutions and $DyVO_4$ should also have the potential to decompose H_2O to H_2 and O_2 by using the same deduction. As for the monoclinic $BiVO_4$, with 2.31 eV band gap, the top of valence band is not located at 2.94 eV versus NHE because the valence band includes the attribution of Bi6s orbital. As reported by A. Kudo

Table 3
Photocatalytic activities of 1 wt% Pt-Cr_2O_3/$Bi_{0.5}M_{0.5}VO_4$ solid solutions for water splitting under UV light irradiation. Catalyst 0.2 g; 300 W Xe lamp as light source; determining and vacuumizing at the interval of 2 h.

Sample	λ > 300 nm	
	H_2 (μmol)	O_2 (μmol)
$Bi_{0.5}Y_{0.5}VO_4$	86.56	44.25
$Bi_{0.5}La_{0.5}VO_4$	61.93	31.08
$Bi_{0.5}Nd_{0.5}VO_4$	22.13	11.26
$Bi_{0.5}Sm_{0.5}VO_4$	75.30	38.16
$Bi_{0.5}Eu_{0.5}VO_4$	10.35	5.6
$Bi_{0.5}Gd_{0.5}VO_4$	26.56	12.89
$Bi_{0.5}Dy_{0.5}VO_4$	67.46	35.29

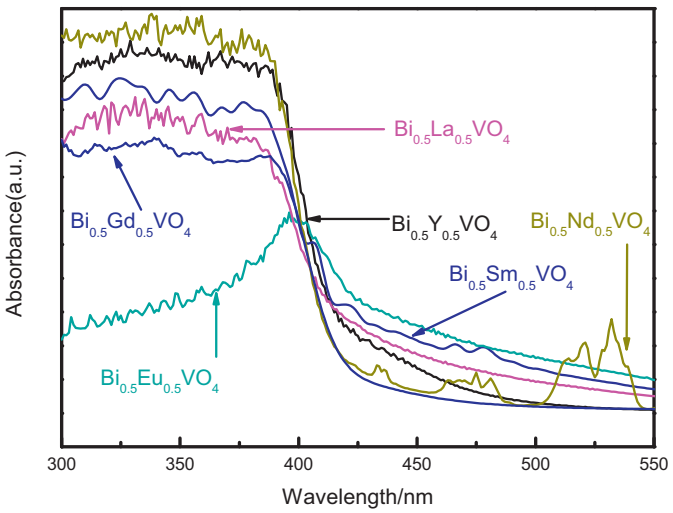

Fig. 9. UV–vis diffuse reflection spectra of $Bi_{0.5}M_{0.5}VO_4$ (M = La, Sm, Nd, Gd, Eu, Y).

[21], the valence band is located at 2.40 eV, lower than the H_2/H_2O potential, so that it has no ability to produce H_2 from H_2O. Based on the observed results about photocatalytic activities of splitting water and the above reasons, a possible band structure of the BDV (0, 0.3, 0.5, 1.0) were shown in Fig. 6. In another paper, the band structure of Bi-based solid solutions was discussed in detail [24].

3.3. Photocatalytic activities of $Bi_{0.5}M_{0.5}VO_4$ (M = La, Sm, Nd, Gd, Eu, Y)

Besides Dy, Y and Lanthanide (La, Sm, Nd, Gd, Eu) also can substitute Bi for forming $Bi_{1-x}M_xVO_4$ solid solutions because of their same charge and similar ion radius. In our study, $Bi_{0.5}M_{0.5}VO_4$ (M = La, Sm, Nd, Gd, Eu, Y) were prepared by solid state reaction. Their structures, the same as $Bi_{0.5}Dy_{0.5}VO_4$, were tetragonal structure (Fig. 7). The SEM photographs of $Bi_{0.5}M_{0.5}VO_4$ (M = La, Sm, Nd, Gd, Eu, Y) solid solutions shown in Fig. 8 indicated these solid solutions were to be irregular-shaped particles and their average particle sizes were about 1–4 μm in diameter. DRS (Fig. 9) indicated $Bi_{0.5}M_{0.5}VO_4$ can absorb a small amount of visible light, and their corresponding absorption edge was about 420 nm. $Bi_{0.5}M_{0.5}VO_4$ (M = La, Sm, Nd, Gd, Eu, Y) also had the photocatalytic activity to split water under UV light when loaded with cocatalyst. The amounts of H_2 and O_2 under UV light irradiation by using 1.0 wt% Pt-Cr_2O_3 loaded $Bi_{0.5}M_{0.5}VO_4$ were shown in Table 3. All of these solid solutions can decompose pure water to the stoichiometrical H_2 and O_2. Among them, $Bi_{0.5}M_{0.5}VO_4$ (M = Dy, Sm, Y) had the best photocatalytic activities. The results indicated that $Bi_{0.5}Y_{0.5}VO_4$ and $Bi_{0.5}Dy_{0.5}VO_4$ had the better photocatalytic activities for overall water splitting, which was probably attributed to the adverse effect of 4f electrons and the ability to absorb visible light, because all of the M elements have 4f electrons or vacant orbit except for Y^{3+}. $Bi_{0.5}M_{0.5}VO_4$ (M = Nd, Gd, Eu) had photocatalytic activities of splitting water, but it could not split water into stoichiometrical H_2 and O_2. This behavior was likely due to the poorer photocatalytic activities which leading to the presence of oxygen in the air.

4. Conclusions

The $Bi_{1-x}Dy_xVO_4$ samples were prepared by solid-state reaction method. The structural and photocatalytic properties of the $Bi_{1-x}Dy_xVO_4$ solid solutions were investigated. The BDV (0.5), the solid solution with an appropriate band gap energy ca.3.01 eV, was discovered to have the best photocatalytic activity to

completely split water into H_2 and O_2 under UV light irradiation when loaded with 1 wt% Pt-Cr_2O_3. Besides, when Bi was substituted by Y and Lanthanide (La, Sm, Nd, Gd, Eu), $Bi_{0.5}M_{0.5}VO_4$ solid solutions loaded with 1 wt% Pt-Cr_2O_3 had the high photocatalytic activities of splitting pure water into H_2 and O_2 under UV light irradiation. By comparing the photocatalytic activities of $Bi_{0.5}M_{0.5}VO_4$ (M = Dy, La, Sm, Nd, Gd, Eu, Y), $Bi_{0.5}Y_{0.5}VO_4$ and $Bi_{0.5}Dy_{0.5}VO_4$ had the best photocatalytic activities for overall water splitting, which was probably attributed to the adverse effect of 4f electrons and the ability to absorb solar light. This study indicated that band-gap engineering of metal oxide solid solutions was the feasible method to simultaneously adjust the CB and VB to obtain stable metal oxide photocatalysts and achieve overall water splitting under UV light irradiation.

Acknowledgements

This work was financially supported by the National Key Basic Research and Development Program (2009CB220000), the Scientific and Technical Innovation Project of Northwest Normal University (nwnu-kjcxgc-03-63), the National Natural Science Foundation of China (20973110) and Gansu Provincial Natural Science Foundation of China (1107RJZA194).

References

[1] A. Fujishima, K. Honda, Nature 238 (1972) 37.
[2] M. Higashi, R. Abe, T. Takata, K. Domen, Chem. Mater. 21 (2009) 1543–1549.
[3] A. Iwase, Y.H. Ng, Y. Ishiguro, A. Kudo, R. Amal, J. Am. Chem. Soc. 133 (2011) 11054–11057.
[4] J. Sato, N. Saito, Y. Yamada, K. Maeda, T. Takata, J.N. Kondo, M. Hara, H. Kobayashi, K. Domen, Y. Inoue, J. Am. Chem. Soc. 127 (2005) 4150–4151.
[5] H.J. Yan, H.X. Yang, J. Alloys Compd. 509 (2011) L26–L29.
[6] K. Maeda, K. Teramura, D.L. Lu, T. Takata, N. Saito, Y. Inoue, K. Domen, Nature 440 (2006) 295.
[7] M.K. Tian, W.F. Shangguan, J. Yuan, L. Jiang, M.X. Chen, J.W. Shi, Z.Y. Ouyang, S.J. Wang, Appl. Catal. A: Gen. 309 (2006) 76–84.
[8] Y.F. Huang, J.H. Wu, Y.L. Wei, J.M. Lin, M.L. Huang, J. Alloys Compd. 456 (2008) 364–367.
[9] S. Tokunaga, H. Kato, A. Kudo, Chem. Mater. 13 (2001) 4624–4628.
[10] L. Jiang, Q.Z. Wang, C.L. Li, J. Yuan, W.F. Shangguan, Int. J. Hydrogen Energy 35 (2010) 7043–7050.
[11] F.X. Zhang, K. Maeda, T. Takata, K. Domen, J. Catal. 280 (2011) 1–7.
[12] H.H. Yang, J.H. Yan, Z.G. Lua, X. Cheng, Y.G. Tan, J. Alloys Compd. 476 (2009) 715–719.
[13] Y.H. Yang, Q.Y. Chen, Z.L. Yin, Jie Li, J. Alloys Compd. 488 (2009) 364–369.
[14] T. Ishii, H. Kato, A. Kudo, J. Photochem. Photobiol. A 163 (2004) 181–186.
[15] D. Li, H. Haneda, S. Hishita, N. Ohashi, Mater. Sci. Eng. B 117 (2005) 67–71.
[16] J. Wang, D.N. Tafen, J.P. Lewis, Z.L. Hong, A. Manivannan, M.J. Zhi, M. Li, N.Q. Wu, J. Am. Chem. Soc. 131 (2009) 12290–12297.
[17] H. Liu, J. Yuan, W.F. Shangguan, Y. Teraoka, J. Phys. Chem. C 112 (2008) 8521–8523.
[18] H.J. Zhang, G. Chen, X. Li, Q. Wang, Int. J. Hydrogen Energy 34 (2009) 3631–3638.
[19] Y. Lee, H. Tetrashima, Y. Shimodaira, K. Teramura, M. Hara, H. Nishiyama, K. Domen, Y. Inoue, J. Phys. Chem. C 111 (2007) 1042–1048.
[20] K. Maeda, N. Sakamoto, T. Ikeda, H. Ohtsuka, A.K. Xiong, D.L. Lu, M. Kanehara, T. Teranishi, K. Domen, Chem. Eur. J. 26 (2010) 7750–7759.
[21] A. Kudo, K. Omori, H. Kato, J. Am. Chem. Soc. 121 (1999) 11459–11467.
[22] H. Liu, J. Yuan, W.F. Shangguan, Y.J. Teraoka, J. Phys. Chem. C 112 (2008) 8521–8523.
[23] Q.Z. Wang, H. Liu, J. Yuan, W.F. Shangguan, Catal. Lett. 131 (2009) 161–163.
[24] H. Liu, J. Yuan, Z. Jiang, W.F. Shangguan, E. Hisahiro, T. Yasutake, J. Mater. Chem. 21 (2011) 16535–16543.
[25] M. Oshikiri, M. Boero, J.H. Ye, Z.G. Zou, G. Kido, J. Chem. Phys. 117 (2002) 7313–7318.
[26] D.E. Scaife, Sol. Energy 25 (1980) 41–54.